

# **FLEXURAL-STRENGTHENING EFFICIENCY OF CFRP SHEETS FOR UNBONDED POST-TENSIONED CONCRETE T-BEAMS**

Long Nguyen-Minh<sup>1</sup>, Phuong Phan-Vu<sup>2</sup>, Duong Tran-Thanh<sup>3</sup>, Quynh Phuong Thi Truong<sup>4</sup>,

Thong M. Pham<sup>5</sup>, Cuong Ngo-Huu<sup>6</sup>, Marián Rovňák<sup>7</sup>

## **ABSTRACT**

There has been a limited number of studies about the flexural behavior of unbonded post-tensioned concrete (UPC) beams strengthened with carbon fibre reinforced polymer (CFRP) and these studies have not systematically examined the effect of CFRP sheets on the tendon strain as well as the strengthening efficiency. Moreover, current design guides for the FRP strengthening techniques have not provided any design procedure for UPC structures. This study, thus, investigates the influence of CFRP sheet ratio on the flexural behavior of CFRP-strengthened UPC T-beams and quantifies its effect upon tendon behavior in this kind of UPC beams. The testing program consisted of nine large-scale UPC T-beams strengthened by different layers of CFRP sheets with or without CFRP U-wrapped anchors. The experimental results have shown that the use of CFRP sheets and CFRP U-wrapped anchors significantly affected the tendon strain. The FRP reinforcement ratio governed the flexural capacity, the crack width, the mid-span displacement, and the ductility of the beams in which the

---

<sup>1</sup>Assoc. Professor, Department of Structural Design, Faculty of Civil Engineering, HCMC University of Technology, 268 Ly Thuong Kiet, District 10, Ho Chi Minh city, Vietnam; Ph.D., Faculty of Civil Engineering, Technical University of Košice, Letná 9, 042 00 Košice, Slovakia. E-mail: [nguyenminhlong@hcmut.edu.vn](mailto:nguyenminhlong@hcmut.edu.vn) (corresponding author).

<sup>2</sup>Ph.D. Student, Department of Structural Design, Faculty of Civil Engineering, HCMC University of Technology, 268 Ly Thuong Kiet, District 10, Ho Chi Minh city, Vietnam, E-mail: [phuong.pv@ou.edu.vn](mailto:phuong.pv@ou.edu.vn)

<sup>3</sup>Research Fellow, BK Structural Engineering Lab, Faculty of Civil Engineering, HCMC University of Technology, 268 Ly Thuong Kiet, District 10, Ho Chi Minh city, Vietnam; E-mail: [tranthanhduong31@gmail.com](mailto:tranthanhduong31@gmail.com).

<sup>4</sup>Lecturer, Van Lang University, 45 Nguyen Khac Nhu, District 1, Ho Chi Minh city, Vietnam; E-mail: [truongthiphuongquynh@vanlanguni.edu.vn](mailto:truongthiphuongquynh@vanlanguni.edu.vn).

<sup>5</sup>Research Fellow, Ph.D., Centre for Infrastructural Monitoring and Protection, School of Civil and Mechanical Engineering, Curtin University, Australia; Lecturer, Department of Structural Design, Faculty of Civil Engineering, HCMC University of Technology, 268 Ly Thuong Kiet, District 10, Ho Chi Minh city, Vietnam. E-mail: [thong.pham@curtin.edu.au](mailto:thong.pham@curtin.edu.au).

<sup>6</sup>Assoc. Professor, Department of Structural Design, Faculty of Civil Engineering, HCMC University of Technology, 268 Ly Thuong Kiet, District 10, Ho Chi Minh city, Vietnam. E-mail: [ngohuucuong@hcmut.edu.vn](mailto:ngohuucuong@hcmut.edu.vn).

<sup>7</sup>Assoc. Professor, Ph.D., Department of Masonry and Concrete Structures, Faculty of Civil Engineering; Technical University of Košice, Letná 9, 042 00 Košice, Slovakia. E-mail: [marian.rovnak@tuke.sk](mailto:marian.rovnak@tuke.sk)

18 strengthening efficiency reduces with the increased number of CFRP layers. The  
19 configuration of the CFRP U-wrapped anchors affected the strain of the CFRP sheets, the  
20 failure mode and thus the beam behavior. In addition, semi-empirical equations were  
21 proposed to estimate the actual strain of unbonded tendons in which the effect of the CFRP  
22 sheets and CFRP U-wrapped anchors have been taken into consideration. The proposed  
23 equations, which are simple to use, yield reliable predictions with a small variation.

24 **Key words:** CFRP sheets; CFRP U-wrapped anchorage; post-tensioned concrete; T-beams;  
25 unbonded tendons; flexural capacity; formula.

## INTRODUCTION

Carbon fiber reinforced polymer (CFRP) has been widely used for strengthening/retrofitting reinforced concrete (RC) structures or post-tensioned concrete (PC) structures. Due to its outstanding properties, such as high strength, low weight, electrical insulator, no magnetic signatures, corrosion resistance, and easy handling, strengthening with CFRP sheets has been showing its excellent performance as compared to other traditional strengthening techniques such as externally epoxy-bonded steel plates or jacketing due to steel corrosion, difficulty in handling the heavy steel plates, increase in dead loads of the structure and labour intensiveness [1]. Early studies about flexurally strengthening RC structures with CFRP sheets started approximately 25 years ago and this topic has been well documented [2-7]. Meanwhile, studies about FRP strengthened PC structures have just recently attracted the research society and these studies mainly focused on PC structures with bonded tendons [8-16]. In particular, the number of studies regarding analysis and evaluation of the FRP-strengthening effectiveness on UPC structures is very limited [17-20]. The lack of experimental results as well as the difficulty in determining the actual strain of unbonded tendons (which are not compatible with surrounding concrete) can be a main reason why a design procedure for such structures has not been introduced in design guides such as ACI 440.2R-17 [21], CNR DT200R1 [22], and TR 55 [23]. In bonded PC beams strengthened with FRP sheets, tendons and surrounding concrete maintain the integrity and thus the strain compatibility condition in tendons, concrete and CFRP reinforcement is satisfied, which leads to a relatively uniform interaction between the tendons and the surrounding concrete along the beams. Nevertheless, this mechanism is not observed in unbonded tendons as there is no bonding between tendons and the nearby concrete. As a result, the interaction of unbonded tendons, the surrounding concrete, and FRP sheets does not uniformly occur along the beam. This difference may lead to a reduction of the flexural strengthening efficiency of

UPC beams as compared to that of PC beams with bonded tendons. Therefore, applications of the design procedure of PC beams with bonded tendons (in many existing design guidelines) to UPC beams could lead to an overestimate of their capacities.

Moreover, thanks to the ability of crack control which reduces crack width and crack spacing in RC beams [24] and PC beams [9], the CFRP sheets have demonstrated the proficiency in increasing the flexural capacity and enhancing the ductility of PC beams [12, 14]. This change in beam behavior results in a slower increase rate and higher maximum values of the tendon strain [13], which indicates that FRP sheets have a considerable influence on the behaviour of tendons. Unfortunately, this influence has not been evaluated quantitatively in the literature, particularly in the case of UPC beams. In addition, the effectiveness of using FRP sheets is governed by its debonding strain [6]. In order to postpone the debonding process and increase the strengthening efficiency, mechanical anchor systems or CFRP U-wrapped anchors have been used and showed high effectiveness for both traditional RC beams [25-29] and PC beams [11, 12]. ACI 440.2R-17 [21] also recommended that properly applying FRP U-wrapped anchors can maximize the actual strain of FRP systems. However, the effect of FRP U-wrapped anchors to FRP-strengthened UPC beams when the number of FRP reinforcement changes has not been presented in the literature.

This study experimentally investigates the flexural behavior of UPC beams strengthened with CFRP sheets and quantifies the effects of the number of CFRP layers and CFRP U-wrapped anchors on the actual strain of the unbonded tendons. The experimental program consisted of nine large-scale CFRP-strengthened UPC T-beams with varied FRP reinforcement ratio and with/without CFRP U-wrapped anchors. In addition, semi-empirical equations were also proposed to determine the strain of unbonded tendons in which the effects of the number of CFRP layers and CFRP U-wrapped anchors have been taken into consideration. The

equations are recommended for estimating the flexural capacity of UPC beams strengthened by CFRP sheets with a high correlation to the experimental results.

## EXPERIMENTAL INVESTIGATION

### *Materials and preliminary tests*

The mixture design of concrete included: Portland cement PC40 (410 kg/m<sup>3</sup>); coarse aggregates (20-22 mm, 1028 kg/m<sup>3</sup>); coarse sands (0÷4 mm, 550 kg/m<sup>3</sup>); fine sands (0÷2 mm, 247 kg/m<sup>3</sup>); and superplasticizer (5.5 l/m<sup>3</sup>). The axial compressive strength and the tensile strength of the concrete determined on 6 concrete cubes 150x150x150 mm were 47.2 MPa (COV=0.02) and 5.8 MPa (COV=0.05) respectively. The slump of the concrete was 120±20 mm. The yield strength  $f_y$ , the ultimate tensile strength  $f_u$  and the rupture strain  $\epsilon_u$  of the longitudinal rebars were  $f_y = 430$  MPa (COV=0.02),  $f_u = 600$  MPa (COV=0.03) and  $\epsilon_u = 21\%$  (COV=0.03) respectively. The corresponding strengths of stirrups were  $f_{yw} = 342$  MPa (COV=0.03) and  $f_{uw} = 463$  MPa (COV=0.01) respectively. The reinforcements had Young's modulus  $E_s = 200$  GPa (COV=0.02). The unbonded tendons were 7-wire strands with the nominal diameter of 12.7 mm. The nominal yield strength  $f_{py}$ , the nominal ultimate strength  $f_{pu}$  and the rupture strain  $\epsilon_{pu}$  of the tendons were  $f_{py} = 1675$  MPa,  $f_{pu} = 1860$  MPa and  $\epsilon_{pu} = 3.5\%$  respectively. The Young's modulus of the tendons was  $E_p = 195$  GPa. The mechanical properties of carbon fiber fabrics (**Fig. 1**) and resin were provided by the manufacturer, in which, the unidirectional CFRP sheet had the nominal thickness of 0.166 mm, the ultimate strength  $f_{ffu} = 4900$  MPa, the elasticity modulus  $E_f = 240$  GPa, and the rupture strain  $\epsilon_{ffu} = 2.1\%$ . The epoxy resin (included two parts, A and B) had the tensile strength  $f_{epoxy,u} = 60$  MPa, the elasticity modulus  $E_{epoxy} = 3$ -3.5 GPa. The mechanical properties of all the materials are presented in **Table 1**.

## 98 *Beam design*

99 The experimental program consisted of nine large-scale UPC T-beams which had the height  
100  $h=360$  mm, the flange width  $b_f=200$  mm, the web width  $b=110$  mm, the flange thickness  
101  $h_f=90$  mm, the beam length  $L_0=6000$  mm, the effective span  $L=5600$  mm, and the concrete  
102 cover was 24 mm as shown in **Fig. 2**. The nine beams included one un-strengthened beam  
103 (beam M0CB) as a reference beam and eight beams strengthened with longitudinal CFRP  
104 sheets as follows: three beams were strengthened with 2, 4, and 6 CFRP layers without CFRP  
105 U-wrapped anchors (beams M2CB, M4CB, and M6CB); three beams were strengthened with  
106 2, 4, and 6 CFRP layers with CFRP U-wrapped anchors non-uniformly distributed within the  
107 shear span (beams M2CB-AN1, M4CB-AN1, and M6CB-AN1); and the remaining two  
108 beams were strengthened with 2 and 4 CFRP layers with CFRP U-wrapped anchors  
109 uniformly distributed within the shear span (beams M2CB-AN2 and M4CB-AN2). The two  
110 different anchorage systems (AN1 and AN2) had the same total cross-sectional area and the  
111 bond area as shown in **Fig. 3**.

112 After 28 days from casting, the beams were post-tensioned by two 7-wire strands (12.7 mm  
113 nominal diameter) with a curved trajectory as shown in **Fig. 2**. The initial jacking force in  
114 each tendon ( $F_{pi}$ ) was 128.5kN. The beams were designed according to ACI 318-14 [30]  
115 Class U with uncracked section. As a requirement, the initial jacking force was determined so  
116 that the following condition is satisfied  $f_t < 0.62(f_c')^{0.5}$ , in which  $f_t$  is the maximum tensile  
117 stress in concrete and  $f_c'$  is the compressive strength of concrete determined from cylinders.  
118 Among these beams, the maximum tensile stress  $f_t = 3.13$  MPa  $< 0.62(f_c')^{0.5} = 3.81$  MPa,  
119 indicating that the above condition is achieved in these beams. The longitudinal steel  
120 reinforcements of the beams included two 12 mm bars in the tension side and four 10 mm  
121 bars in the compression side. Stirrups had the diameter of 6 mm at a spacing of 175 mm and

were uniformly distributed along the beams except the two ends (250 mm) where a spacing of 50mm was used to avoid possible local damages. More details and the test parameters are presented in **Table 2** while the beam design and the strengthening schemes are shown in **Figs. 2 and 3**.

The installation of CFRP sheets were conducted one day after tensioning the beams. Before bonding with CFRP sheets, the concrete surface was ground with an angle grinder until touching aggregates. Any holes or imperfection on the concrete surface were filled with epoxy and then grounded off. A vacuum machine was used to clean any dust on the concrete surface which also was checked again carefully before bonding. Epoxy was mixed according to the instruction provided by the manufacturer and a thin layer of epoxy was spread on the concrete surface by a roller before placing the first layer of the CFRP sheet. Another epoxy layer was then spread on top of the first CFRP sheet while just-enough pressure was applied via the roller so that the CFRP sheet was saturated. The roller was rolled gently on top of the applied CFRP sheets to ensure there was no air bubble in the composite matrix. The wrapping process was carried out in the laboratory at the average temperature of 28°C and the humidity of 75%. The strengthened beams were left in the laboratory for 7 days during the curing period to ensure that the strength of the epoxy was fully developed. The beams were tested right after this period. All the beams were stored in the laboratory during the period from casting to testing.

### ***Test procedure and instrumentation***

All the beams were tested until failure under four-point bending tests as shown in **Fig. 3**. The applied load location was beyond the nearest support at about  $L/3 = 1870$  mm. The actual strain of the CFRP sheets was monitored by using strain gauges (SG) which were bonded on the surface of the CFRP sheets at the midspan, the loading points and within the shear span.

The tendon strain was measured by five SGs which located at the anchorages, the midspan, and the loading points. Strain of the rebars was measured by one SG bonded at the midspan while strain of concrete was monitored by five SGs with the gauge length of 60 mm which were surface mounted along the height of beam section, as shown in **Fig. 3**. Strain of CFRP U-wrapped anchors was measured by four SGs bonded onto two U-wraps nearest to the loading points. In addition, the displacements of the beams were measured by five linear variable differential transformers (LVDTs) which were placed at the midspan, the loading points, and the supports. The beams were tested under the force controlled scheme in which the load step of 15 kN was applied before cracking and the load step of 30 kN was utilized afterwards. After reaching each load step, the load was maintained in 3 minutes to record the displacements and strain.

## TEST RESULTS AND DISCUSSION

### *Failure mode*

The reference beam showed a flexural failure with yielding of the tendons and damage of the concrete in the compressive zone after that as shown in **Fig. 4a**. The failure of the reference beam showed a more brittle manner than that of the strengthened beams, as evident from faster crack development, less number of cracks but wider crack widths. The first flexural crack appeared at the mid-span associated with a load of about 32% of the maximum load.

The maximum crack width measured at the maximum load was approximately 1.8 mm.

The strengthened beams also failed in the flexural manner in which the tendons yielded before debonding or rupturing of the CFRP sheets as shown in **Figs. 4b-i**. The concrete damage at the compression zone was less severe than that of the reference beam and the damage locally occurred at the loading points. The failure of the strengthened beams showed a less brittle manner with more number of cracks and smaller crack widths. The first flexural



crack in FRP-strengthened beams occurred at an average load of 29%-30% of the maximum load. Using the CFRP sheets significantly increased the cracking load,  $P_{cr,exp}$ , of the strengthened beams by 7%-26% in comparison to that of the reference beam. The cracking-load enhancement increased with the number of CFRP sheets. Interestingly, the CFRP U-wrapped anchors did not have an influence on the cracking load of the tested beam. A cracking sound indicating the debonding of the CFRP sheets was heard at about 90% the maximum load. There were two typical debonding mechanisms including cover delamination in the flexural span and interfacial debonding in the shear span as shown in **Fig. 5**. The maximum crack widths of the strengthened beams ranged from 0.8 mm to 1.4 mm which were 45%-78% of maximum crack width of the reference beam.

The CFRP U-wrapped anchors significantly changed the failure modes of the CFRP sheets. All the longitudinal CFRP sheets of the strengthened beams without the CFRP U-wrapped anchors debonded at the maximum loads while the longitudinal CFRP sheets of the strengthened beams with the anchors either ruptured or debonded. For the strengthened beams with the uniformly distributed anchors type AN2, all the longitudinal CFRP sheets ruptured at the maximum load as shown in **Figs. 4h-i**. On the other hand, for the beams with the anchors type AN1, the rupture of the longitudinal CFRP sheets was just observed with beam M2CB-AN1 which was strengthened by two layers of CFRP sheets (**Fig. 4e**). This observation has shown that the anchor configuration and the relation between the axial stiffness of the CFRP anchor system and the longitudinal CFRP sheets governed the failure mode of the longitudinal CFRP sheets. The anchor system type AN1 was designed to have CFRP U-wrapped anchors concentrated at the supports, which was expected to delay the slipping and the debonding of the longitudinal CFRP sheets at the beam ends. However, this configuration (type AN1) had the spacing between U-wraps greater than that of type AN2 and thus increased stress in each single U-wrap (**Table 3**) and therefore reduced its efficiency,

particularly for those close to the loading points. As a result, the U-wraps close to the loading points failed prior to the others when the applied load was approaching the maximum load. Once the first U-wrap failed, stress in the longitudinal CFRP sheets concentrated on the next U-wrap and caused a progressive failure of the whole anchor system. Accordingly, the longitudinal CFRP sheets debonded at the maximum load. For the beams with the anchor system type AN2, the U-wraps were evenly distributed associated with a smaller spacing and thus the strain in the U-wraps was smaller as presented in **Table 3**. The measured strain in these U-wraps was far smaller than the rupture strain of the material so that the longitudinal CFRP sheets did not debond at the anchorage zone but shifted to the rupture failure mode at the flexural span.

The debonding mechanism in the tested beams included cover delamination and interfacial debonding which both occurred in the same beam as shown in **Fig. 5**. These debonding mechanisms were discussed in previous studies by Smith and Teng [31], Teng et al. [32], [33], in which the cover delamination was observed near the end of FRP sheets while the interfacial debonding usually occurs in the flexural span as also mentioned in ACI 440.2R-17 [21]. It is noted that these observations were based on RC beams without U-wraps. However, the location of the debonding of the UPC beams in this study was different from the previous studies, in which the cover delamination was observed in the flexural span (between the two loading points) while the interfacial debonding occurred within the shear span. In the flexural span, large tensile stress caused flexural cracks and reduced the bond strength between the longitudinal rebars and the surrounding concrete. As the applied load increased, the flexural cracks widened and led to relative slippage between the longitudinal rebars and concrete cover. Concrete teeth associated with splitting cracks were observed along the longitudinal axis of the rebars within the flexural span. When the applied load was approaching the maximum load, the splitting cracks interacted each other and were wide enough to cause the

cover delamination in which the concrete cover at the soffit separated from the beam. Meanwhile, the tensile stress at the beam soffit and the crack width within the shear span were much smaller than those at the flexural span. As a result, losses of the bonding and the relative slippage between the longitudinal rebars and the surrounding concrete were much smaller than those at the flexural span. At higher load level, the tensile stress in this region might have exceeded the shear strength of the resin-concrete interface but this stress was not big enough to cause slippage of the rebars and thus the interfacial debonding occurred in the shear span.

#### *Load – deflection relationships and flexural capacity*

The behavior of the tested beams was analyzed at three different load levels at: the cracking loads, the allowable load at the serviceability state, and the maximum loads. The load-deflection relationship of the tested beams showed a linear behavior up to the cracking load of the reference beam ( $P_{cr,0}$ ),  $M_0 (P_{cr,0} = 0.32 P_{u,0}$ , where  $P_{u,0}$  is the maximum load of the reference beam), and there was no difference in the load-deflection curves as shown in **Fig. 6**. During this period, the CFRP sheets and the tendons had almost no influence on the beam behavior. However, once the applied load was greater than the cracking load of the reference beam ( $P_{cr,0}$ ), the crack development led to a degradation of the stiffness and thus the beam deflection increased with a higher rate, in which the deflection increase of the strengthened beams was much smaller than that of the reference beam. Meanwhile, the flexural-strengthening CFRP sheets showed their role in delaying the crack development and postponing the degradation of the stiffness of the strengthened beams. As a result, the strengthened beams showed a smaller deflection than that of the reference beam at the same applied load.

When the applied load increases to a load level which causes the displacement equal to the allowable displacement ( $L/250 = 22.5$  mm) at the serviceability state, the applied load of the reference beam was  $P_{ser,0} = 0.52P_{u,0}$ . This value is then called the allowable load at the serviceability state ( $P_{ser}$ ). At  $P_{ser,0}$ , the displacement of the beams strengthened with 2, 4 and 6 CFRP layers reduced by 16%-29%. Similarly, at the load level of the maximum load of the reference beam  $P_{u,0}$ , a reduction by 9%-31% was observed for the displacement of the strengthened beams as compared to that of the reference beam. At the same load level, the more number of CFRP layers was applied, the less displacement was observed; this reduction, however, became smaller with more number of CFRP layers. On the other hand, the maximum displacement of the strengthened beams increased significantly as compared to that of the reference beam, for instance, 9%-54% for the beams without anchors and 20%-65% for the beams with anchors as shown in **Fig. 7b**, but the increase rate reduced with more CFRP layers.

In addition, the strengthened beams showed higher energy absorption capacity ( $E_b$ ) regarding the reference beam as shown in **Table 3**. The energy absorption capacity ( $E_b$ ) was calculated by the area under the load-displacement curves up to the maximum loads (**Fig. 8**). In comparison with the reference beam, the energy absorption capacity of the strengthened beams increased from 41% to 144% and from 23% to 94% for strengthened beams with and without anchors, respectively (**Table 3**). The strengthened beams with anchors exhibited considerably higher energy absorption capacity than those without anchors.

The strengthened beams exhibited significantly higher flexural capacity than that of the reference beam and the capacity increased with the number of CFRP layers but this increase has slowed down when more number of CFRP layers was used. At the force level of  $P_{ser,0}$  (at serviceability state), the displacement of the strengthened beams slightly reduced by 8%-17%.

During this period, the anchor system did not show a considerable influence on the displacement of the strengthened beams. Up to the ultimate load, the CFRP sheets significantly affected the performance of the strengthened beams, for example, the increase in flexural capacity of strengthened beams ranged from 8%-31% for the beams without anchors and 17%-37% for those with anchors as shown in **Fig. 7a**. During this period, the CFRP U-wrapped anchor system eliminated the relative slippage and debonding of the CFRP sheets and thus considerably enhanced the FRP-strengthening effectiveness and the flexural capacity of the beams as well. In addition, the effect of the anchor systems AN1 and AN2 on the flexural capacity of the tested beams was quite similar.

### **Cracking behaviour**

The experimental results have shown that the flexural-strengthening CFRP sheets could significantly arrest cracks and delay the crack development, as shown in **Fig. 9**. The more CFRP layers were used, the smaller crack widths were observed. Cracking behaviour of the tested beams was quite similar; however, cracks in the beams without the CFRP U-wrapped anchors developed faster than in those with the CFRP U-wrapped anchors. The flexural cracks of the strengthened beams appeared later than those of the reference beam. The cracking loads of the strengthened beams ( $P_{cr,CFRP}$ ) were greater than that of the reference beam: 11%-26% and 7%-26% for the beams with and without the CFRP U-wrapped anchors respectively (**Table 3**). At the failure load of the reference beam ( $P_{u,0}$ ), crack widths of the strengthened beams were smaller than that of the reference beam. The differences varied from 2.5 to 3.6 times for beams with anchors and from 2.8 to 3.6 times for beams without them. The reduction of the crack widths became smaller as the number of CFRP reinforcement layers increased (**Fig. 10a**). Cracking was more restricted because of the increasing CFRP axial stiffness ( $E_f A_f$ ), in which  $E_f$  and  $A_f$  are the elastic modulus and the

cross-sectional area of the CFRP sheets respectively. Similarly, the maximum crack width of the strengthened beam was also significantly smaller regarding the reference beam: from 1.3-1.6 times for the beams with anchors and from 1.3-2.3 times for those without them as shown in Fig. 10b.

### *Strain in CFRP sheets and concrete*

The relationships between the load and strain of the CFRP sheets are shown in Fig. 11. Before the cracking load of the beams ( $0.34\sim0.40 P_{u,0}$ ), the strain of the CFRP sheets was small and it was not dependent on the number of the CFRP layers and the anchor system. After the cracking loads, the strain of the CFRP sheets increased significantly, but the increase was reduced when more CFRP layers were applied. The increase rates of strain in the CFRP sheets with and without anchors were almost similar but the maximum strain of CFRP sheets with anchors were much higher than its counterpart in those without anchors. In addition, the strain of the CFRP sheets at the loading points was higher than that at the mid-span.

The maximum strain of the CFRP sheets in the beams without anchors strengthened with 2, 4, and 6 layers was 12.4‰, 11.5‰, and 8.1‰, which corresponded to 59%, 55%, and 38% the rupture strain from coupon tests ( $\varepsilon_{fu}=21\%$ ), respectively. For the beams with the anchor system AN1, the maximum strain of CFRP sheets slightly increased (12%-17%) as compared to those without anchors and this enhancement tended to reduce with more CFRP layers, for instance, strain of the CFRP sheets of beams M2CB-AN1, M4CB-AN1, and M6CB-AN1 was 14.5‰, 12.9‰, and 9.5‰, corresponding to 69%, 61%, and 45% the rupture strain of the CFRP sheets, respectively. Meanwhile, the strain of the CFRP sheets of beams M2CB-AN2 and M4CB-AN2 was 13.9‰ and 11.5‰ which corresponds to 66% and 54% the rupture

strain of the CFRP sheets, respectively. The strain was reduced about by 34% and 12% when the number of CFRP layers increased from 2 to 6 layers, and from 2 to 4 layers, respectively.

As shown in **Fig. 11**, the maximum strain of the CFRP sheets reduced with the increase of the number of CFRP layers which resulted in a higher stiffness of the CFRP sheets. In addition, the CFRP U-wrapped anchors had shown their effectiveness in eliminating the relative slippage and debonding of the CFRP sheets and thus increased the strengthening efficiency, as evident from the increase of the CFRP strain of the beams with anchors in comparison with those without anchors. It is worth mentioning that the strain of the CFRP sheets of the reference beam at the loading points was considerably greater (up to 93%) than that at the mid-span. The difference in strain of the CFRP sheets in flexural span could be due to the phenomenon of the stress concentration occurred at the loading points. On the other hand, the mentioned difference in strains of CFRP sheets of the strengthened beams with anchors was smaller: 18%-26% for the beams with the anchor system AN1; and about 5% for the beams with the anchor system AN2. It is obvious that using CFRP U-wrapped anchors leads to more uniformly distributed strain in the CFRP sheets, particularly for the beams with the anchor system AN2.

Furthermore, the use of the CFRP sheets significantly affected also the compressive concrete strain. As mentioned previously, the CFRP sheets were able to arrest cracks and delay their development as shown in **Fig. 9**. This phenomenon led to a greater height of the compressive concrete zone for the strengthened beams as compared to that of the reference beam at the same loading level, which resulted in lower concrete strain in the strengthened beams. For instance, at the maximum load, strain of the compressive concrete of the reference beam was 3.5‰ while the corresponding strain of the strengthened beams was 1.9‰-2.7‰ for the strengthened beams without anchors (23%-46% reduction) and 2.4‰-3.0‰ for those with

anchors (14%-31% reduction) as presented in **Table 3**. It is noted that the reduction of the concrete strain of the strengthened beams reduces when the number of the CFRP layers increases. This phenomenon can be explained from the efficiency of the CFRP sheets in reducing the crack width as previously discussed and shown in **Fig. 10b**.

#### *Strain in tendons and effect of CFRP sheets*

Before the occurrence of the first crack, the tendons did not really contribute to the flexural resistance due to the small strain increases ( $< 0.35\%$ ). It is noted that the tendon strain increase was estimated by deducting the initial post-tensioning strain ( $5.16\%$ ) from the actual strain. During this phase, the behavior of the tendons was quite similar among the tested beams. After cracking of the beams (about  $0.4P_{u,0}$ ), the strain of the tendons started to increase considerably. The tendon strain increase in the strengthened beams was smaller than those in the reference beam, and this tendon strain increase was slowed down when more CFRP layers or anchors were used (**Fig. 11**).

At the allowable load at the serviceability state of the reference beam, the increase in the tendon strain in beam M0 was about  $1.5\%$  while the corresponding increase in tendon strains in strengthened beams without anchors, namely, M2CB (2 CFRP layers), M4CB (4 layers), and M6CB (6 layers) was  $1.4\%$ ,  $1.3\%$ , and  $1.2\%$  respectively, which showed a reduction of  $7\%$ ,  $14\%$  and  $20\%$  respectively, in comparison with the reference beam. Similarly, the reduction of the tendon strain increase in the strengthened beams with anchors was  $18\%$ ,  $22\%$ , and  $24\%$  for beams M2CB-AN1 (2 CFRP layers), M4CB-AN1 (4 layers), and M6CB-AN1 (6 layers), respectively, and  $12\%$  and  $19\%$  for beams M2CB-AN2 (2 layers) and M4CB-AN2 (4 layers), respectively, as compared to that in the reference beam.

In the loading phase after the allowable load at the serviceability state, the tendon strain increase in the strengthened beams was much smaller than that in the reference beam at the



same loading level. For instance, at the maximum load of the reference beam ( $P_{u,0}$ ), the tendon strain increase in the strengthened beams without anchors M2CB (2 CFRP layers), M4CB (4 layers), and M6CB (6 layers) was smaller by 23%, 40%, and 50% respectively. The tendon strain increase in the strengthened beams with anchor system AN1, M2CB-AN1 (2 CFRP layers), M4CB-AN1 (4 layers), and M6CB-AN1 (6 layers) was smaller by 34%, 47%, and 50% respectively. Similarly, the corresponding reduction of the tendon strain increase in the strengthened beams with anchor system AN2, M2CB-AN2 (2 layers) and M4CB-AN2 (4 layers) was smaller by 30% and 46% respectively.

On the other hand, the flexural-strengthened CFRP sheets led to a significant greater strain increase of the tendons at the maximum load regarding the reference beam: from 11% to 18% for the strengthened beams without anchors; and from 25% to 60% for those with anchors (Fig. 12). The reduction rate of CFRP sheet strain was faster than the increase rate of tendon strain at the failure load as the number of CFRP layers rose, which was clearly presented in Fig. 13. These results have shown that the maximum strain of the CFRP sheets was more sensitive to the number of CFRP layers than the tendon strain increase at the maximum loads. In addition, in terms of 2 layers of CFRP sheet and without anchors, the maximum tendon strain increase was quite similar to those in the reference beam (3.79‰ and 3.77‰, respectively); however, when it comes to 4 and 6 layers of CFRP sheet, the tendon strain increase was significantly greater and more uniformly.

The above results and analyses have proven that the CFRP sheets and the CFRP U-wrapped anchors have strong influences on the behavior of the tendons. As previously mentioned, the CFRP sheets were able to arrest cracks and prevent the crack development and they slowed down the degradation of the beam stiffness. The tensile stress in the beams was more uniformly distributed and thus this phenomenon minimized possible localized damage in

concrete and the tendons, which helped to reduce the strain in tendons and, more importantly, helped to delay the occurrence of the yielding of tendons as presented in **Fig. 11**. Accordingly, using 2, 4, and 6 layers of CFRP increased the yielding loads by 7.7%, 13.8%, and 24.1% for the beams without anchors and 12.8%, 25.1%, and 31.3% for those with anchors regarding the reference beam, respectively (**Fig. 14**). It is noted that the tendons in all tested beams exceeded the yield strain at the ultimate loads ( $\epsilon_{py} = f_{py}/E_p = 1675/195 = 8.59\%$ ).

### *Parameters reflecting the CFRP strengthening action in strain of tendons*

The above discussions have shown that the number of CFRP layers (indicating the axial stiffness of the CFRP sheets) and their maximum actual strain significantly affect the strain increase of the tendons (**Figs. 11-13**). The correlations between the ratio of the strain increase of the tendons of the strengthened beams to that of the reference beam ( $\Delta\epsilon_{ps,CFRP}/\Delta\epsilon_{ps,0}$ ) and three factors  $p_1$ ,  $p_2$  and  $p_3$  related to CFRP sheets are shown in the **Fig. 15**. The factors were specified as follows: (1) the axial stiffness ratio,  $p_1 = E_f A_f / (E_c A_c)$ , where  $E_f$  and  $A_f$  are the elasticity modulus and the cross-sectional area of the CFRP sheets, respectively;  $E_c$  and  $A_c$  are Young's modulus of concrete and the cross-sectional area of the beam, respectively; (2) the FRP efficiency factor,  $p_2 = \epsilon_{fu} / \epsilon_{ffu}$ , where  $\epsilon_{fu}$  and  $\epsilon_{ffu}$  are the actual maximum strain and the rupture strain from coupon tests of the CFRP sheets, respectively; and (3) the combination of the factors  $p_1$  and  $p_2$ ,  $p_3 = 1 + 100p_1p_2$ . According to Maguire et al. [34], if absolute of the correlation coefficient (CORR) is close to 1, two variables have a strong linear relationship while if absolute of CORR is less than 0.2, two variables have a very weak statistical linear correlation. In the study, the sample Pearson correlation coefficient was used. If the variable  $x$  have a dataset  $\{x_1, x_2, \dots, x_{ns}\}$  comprising  $ns$  values and the variable  $y$  have a dataset  $\{y_1, y_2, \dots, y_{ns}\}$  comprising  $ns$  values, the correlation coefficient of  $x$  and  $y$  is determined as follows:

410

$$r_{xy} = \frac{\sum_{i=1}^{ns} (x_i - \bar{x})(y_i - \bar{y})}{\sqrt{\sum_{i=1}^{ns} (x_i - \bar{x})^2} \sqrt{\sum_{i=1}^{ns} (y_i - \bar{y})^2}} \quad (1)$$

411

where  $ns$  is the sample size;  $x_i$  and  $y_i$  are the sampling units indexed with  $i$  of variable  $x$  and  $y$

412

respectively;  $\bar{x}$  and  $\bar{y}$  are the sample mean of variable  $x$  and  $y$  respectively.

413

From **Fig. 15a**, the strain increase of the unbonded tendons has a strong correlation with the

414

factor  $p_1 = E_f A_f / (E_c A_c)$ , in which the correlation coefficient is equal to **1.0** for the beams

415

without anchors and 0.98 for those with anchors. When the number of the CFRP layers

416

increased from 2 to 6, the tendon strain increase was directly proportional to the factor  $p_1$ .

417

Similarly, the tendon strain increase **was** inversely proportional to the factor  $p_2 = \varepsilon_{fu} / \varepsilon_{ffu}$ , with

418

CORR= -0.89 and -0.97 for the beams with and without anchors, respectively (**Fig. 15b**).

419

In general, determining the influence of the CFRP sheets **on** the strain increase of tendons by

420

using the two independent factors  $p_1$  and  $p_2$  may not provide a complete analysis. For

421

instance, the factor  $p_1$  reflects the effect of the axial stiffness of CFRP sheets but it does not

422

consider the actual strain in the CFRP sheets. In reality, the actual strain of CFRP sheets is

423

usually smaller than the rupture strain determined from coupon tests as it is governed by the

424

debonding strain of the CFRP sheets. On the other hand, factor  $p_2$  just represents the actual

425

working capacity of CFRP sheets but **it does not express** the influence of the **relative** axial

426

stiffnesses **of both** the CFRP sheets and the beam. **Therefore, the factor  $p_3 = 1 + 100p_1p_2$  was**

427

**suggested in order to have a more appropriate reflection of the effect of CFRP sheets on**

428

**tendon strain increase**. Correlation analysis for this factor,  $p_3$ , produced good results with

429

CORR=0.94 for the beams with anchors and CORR=0.88 for those without anchors (**Fig.**

430

**15c**).

## PROPOSED FORMULA

### *Strain increase of the tendons*

In order to estimate the flexural capacity of UPC beams strengthened with FRP sheets, determining the strain increase of unbonded tendons is a key issue. Unfortunately, the design guidelines, such as TR 55 [23], CNR DT200R1 [22], and ACI 440.2R-17 [21], have only suggested a procedure to calculate the strain increase of bonded tendons in PC beams strengthened with FRP sheets while the corresponding procedure for unbonded tendons has not been mentioned. In addition, the experimental results have shown that FRP sheets significantly affect the behavior of the unbonded tendons. Therefore, it is not appropriate to directly use either the procedure for PC beams strengthened with FRP and bonded tendons or normal RC beams with unbonded tendons for the beams in this study.

The tendon strain increase of the UPC beams strengthened with FRP was estimated by using the equation suggested by Tam and Pannell [35] for unbonded tendons in normal RC beams, implementing the factor  $p_3$  as follows:

For beams **without** FRP U-wrapped anchors:

$$\Delta \varepsilon_{ps,CFRP} = \psi \varepsilon_c \left( \frac{d_p - c}{L_0} \right) \times \left( 1 + 100 \frac{A_f E_f}{A_c E_c} \frac{\varepsilon_{fe}}{\varepsilon_{ffu}} \right)^{0.59} \quad (2)$$

For beams **with** FRP U-wrapped anchors:

$$\Delta \varepsilon_{ps,CFRP} = \psi \varepsilon_c \left( \frac{d_p - c}{L_0} \right) \times \left( 1 + 100 \frac{A_f E_f}{A_c E_c} \frac{\varepsilon_{fe}}{\varepsilon_{ffu}} \right)^{1.35} \quad (3)$$

The total **strain** of the unbonded tendons  $\varepsilon_{ps,CFRP}$  is then estimated as follows:

$$\varepsilon_{ps,CFRP} = \varepsilon_{pe} + \Delta \varepsilon_{ps,CFRP} \quad (4)$$

Here  $\varepsilon_{pe}$  is the initial strain of a tendon excluding stress losses  $=F_p/(E_p A_p)$  where  $F_p$  (N) is the actual tension force in a tendon;  $E_p$  (N/mm<sup>2</sup>) and  $A_p$  (mm<sup>2</sup>) is the elasticity modulus and cross-sectional area of a tendon, respectively;  $\Delta\varepsilon_{ps,CFRP}$  is the strain increase of tendons;  $\psi$  is the ratio of the length of the plastic zone to the height of the compressive concrete zone:  $\psi=21.4$  according to a study by Au and Du [36] for simply supported UPC beams which are un-cracked and strengthened with CFRP, and  $\psi=9.8$  regarding a study by El Meski and Harajli [19] for the pre-cracked UPC beams strengthened by CFRP sheets;  $\varepsilon_c$  is the strain at extreme concrete compression fiber according to ACI 440.2R-17 [21];  $d_p$  (mm) is the distance from the farthest point of the compressive concrete zone to the centroid of tendon cross-sectional area;  $c$  (mm) is the height of the compressive concrete zone according to ACI 318-14 [30];  $L_0$  (mm) is the length of the beams; and  $\varepsilon_{fe}$  is the actual strain in CFRP sheets at the maximum load.

#### *Evaluation of the proposed formula*

The proposed Eqs. (2), (3), and (4) were implemented to the calculation of flexural capacities of the 24 UPC beams strengthened with CFRP sheets including the 8 beams tested in this study and 16 beams and slabs from the study by El Meski and Harajli [18]. The predicted flexural capacity,  $M_{u,pred}$ , was calculated according to ACI 440.2R-17 [21] with the materials and strength reduction factors considered to equal 1.0, as follows:

*1<sup>st</sup> Step – Estimation of the depth of the compressive concrete zone,  $c$*

The depth to neutral axis,  $c$  (mm), is first assumed, which may be  $0.1h$  as suggested by ACI 440.2R-17 [21], where  $h$  is the height of the concrete cross-section.

*2<sup>nd</sup> Step – Calculation of the strain in CFRP sheets, concrete and tendons*

(a) The strain in CFRP sheets,  $\varepsilon_{fe}$ , for failure dictated by concrete crushing:

$$\varepsilon_{fe} = \varepsilon_{cu} \left( \frac{d_f - c}{c} \right) - \varepsilon_{bi} \leq \varepsilon_{fd}, \quad (5)$$

where  $d_f$  is the effective depth of CFRP sheets,  $\varepsilon_{cu}$  is the ultimate compressive strain of concrete,  $=0.003$ ,  $c$  is the depth of the compressive concrete zone,  $\varepsilon_{bi}$  is the initial substrate strain:

$$\varepsilon_{bi} = \frac{-F_p}{E_c A_c} \left( 1 + \frac{e y_b}{r^2} \right) + \frac{M_{DL} y_b}{I_c A_c}, \quad (6)$$

where  $F_p$  (N) is the effective prestressing force;  $e$  (mm) is the eccentricity of the prestressing force with respect to the centroid of the concrete cross-section;  $y_b$  (mm) is the distance from the centroidal axis of gross-section, neglecting reinforcement, to the extreme bottom fiber;  $r$  (mm) is the radius of gyration of the section,  $=(I_c/A_c)^{0.5}$ ;  $I_c$  (mm<sup>4</sup>) is the second moment of concrete cross-sectional area with respect to an axis passing through its centroid;  $M_{DL}$  (Nmm) is the moment due to dead load of the beam;  $\varepsilon_{fd}$  is the debonding strain as:

$$\varepsilon_{fd} = 0.41 \sqrt{\frac{f'_c}{n E_f t_f}} \leq 0.9 \varepsilon_{ffu}, \quad (7)$$

where  $f'_c$  is the concrete strength,  $E_f$ ,  $t_f$  and  $\varepsilon_{ffu}$  is the elasticity modulus, thickness and the rupture strain of carbon fiber fabric, respectively; and  $n$  is the number of CFRP layers.

(b) The strain in CFRP sheets,  $\varepsilon_{fe}$ , for failure dictated by prestressing steel rupture:

$$\varepsilon_{fe} = \left( \varepsilon_{pu} - \varepsilon_{pi} \right) \left( \frac{d_f - c}{d_p - c} \right) - \varepsilon_{bi} \leq \varepsilon_{fd}, \quad (8)$$

where  $\varepsilon_{pu}$  is the rupture strain of tendons ( $=0.035$ ),  $\varepsilon_{pi}$  the initial strain in tendons, which can be calculated as:

$$\varepsilon_{pi} = \frac{F_p}{A_p E_p} + \frac{F_p}{A_c E_c} \left( 1 + \frac{e^2}{r^2} \right) \quad (9)$$

*3<sup>rd</sup> Step – Calculation of the strain in steel rebars*

The strain in steel rebars,  $\varepsilon_s$ :

$$\varepsilon_s = (\varepsilon_{fe} + \varepsilon_{bi}) \left( \frac{d - c}{d_f - c} \right) \text{ for tensile rebars} \quad (10)$$

$$\varepsilon_s' = (\varepsilon_{fe} + \varepsilon_{bi}) \left( \frac{c - d'}{d_f - c} \right) \text{ for compressive rebars} \quad (11)$$

4<sup>th</sup> Step – Recalculation of the depth of compressive concrete zone,  $c$ :

From the force equilibrium, the depth of compressive concrete zone,  $c$ , is re-computed as follows:

$$c = \frac{(A_p f_{ps} + A_s f_s + A_f f_{fe} - A_s' f_s')}{\alpha_1 f_c' \beta_1 b}, \quad (12)$$

where  $f_{fe}$  (N/mm<sup>2</sup>) is the stress in CFRP sheets,  $=E_f \times \varepsilon_{fe}$ ;  $f_{ps}$  (N/mm<sup>2</sup>) is the stress in tendons,  $=E_p \times \varepsilon_{ps,CFRP} \leq f_{py}$ ;  $f_s$  (N/mm<sup>2</sup>) is the stress in tensile rebars,  $=E_s \times \varepsilon_s \leq f_y$ ; and  $f_s'$  (N/mm<sup>2</sup>) is the stress in compressive rebars,  $=E_s \times \varepsilon_s' \leq f_y$ .

5<sup>th</sup> Step – Checking of the depth of compressive concrete zone,  $c$ :

If the assumed value of  $c$  ( $c_{assu}$ ) and re-calculated one ( $c_{cal}$ ) meet the convergence criterion as presented in Eq. 13, the proper value of  $c$  is attained; if not, the re-calculated value of  $c$  or an average value of assumed and re-calculated value of  $c$  is re-chosen and the process starting at 2<sup>nd</sup> step is iterated until convergence is reached.

$$\text{convergence criterion} = \frac{|c_{assu} - c_{cal}|}{c_{assu}} \leq 0.1\% \quad (13)$$

6<sup>th</sup> Step – Calculation of the flexural capacity of CFRP-strengthened beam

Finally, the flexural capacity of CFRP-strengthened UPC beam,  $M_{u,pred}$ , can be estimated according to Eq. (14):

$$M_{u,pred} = A_p f_{ps} \left( d_p - \frac{\beta_1 c}{2} \right) + A_f f_{fe} \left( d_f - \frac{\beta_1 c}{2} \right) + A_s f_s \left( d - \frac{\beta_1 c}{2} \right) + A_s' f_s' \left( \frac{\beta_1 c}{2} - d' \right) \quad (14)$$

All symbols used in Eqs. 1-14 are in List of Symbols. The ratios of predicted to experimental flexural capacities  $M_{u,pred}/M_{u,exp}$  are summarized in the Table 4 and Fig. 16. The mean value Mean=0.94 and coefficient of variation COV=0.07 indicated the accuracy of theoretical

tendon strain values and their appropriateness for prediction of the flexural capacity of the CFRP strengthened UPC beams with and without CFRP U-wrapped anchors.

## CONCLUSIONS

The effect of CFRP sheets and CFRP U-wrapped anchors on the unbonded tendons and the flexural behavior of UPC T-beams were investigated and quantified in the study. From the experimental results, the following findings can be summarized as follows:

1. The flexural-strengthening efficiency of CFRP sheets for the UPC beams was governed by the CFRP sheet ratio. The use of CFRP sheets led to the considerable increase of the flexural capacity of the UPC beams (up to 37%); however, this enhancement tended to decrease as CFRP sheet ratio increased. In addition, the cracking load increased up to 26%, the crack widths were also significantly reduced up to 1.55 times and 3.6 times at the serviceability and ultimate state, respectively. The maximum displacement and the energy absorption of strengthened UPC beams also increased up to 60% and 144%, respectively;
2. The CFRP sheets and CFRP U-wrapped anchors significantly affect the behavior of the tendons. At the same loading level, the strain increase of the tendons in the strengthened beams was much smaller than that of the reference beam from 23% to 50%. Besides, the use of CFRP sheets also increased the maximum strain increase of the tendons from 11% to 18% for the beams without anchors and from 25% to 60% for those with anchors. This increase is directly proportional to the number of CFRP layers;
3. The CFRP sheet ratio and CFRP U-wrapped anchors governed the failure mode of the UPC beams. The CFRP debonding was observed in the strengthened beams without U-wrapped anchors while CFRP rupture was observed in those with U-wrapped anchors. The CFRP U-wrapped anchors slightly improved the flexural capacity and displacement of the beams but significantly increased strain of the CFRP sheets (18%);



4. The strain of the CFRP sheets was inversely proportional to the number of CFRP layers. The maximum strain of the CFRP sheets ranged from 8.1‰ to 12.4‰ (from 38% to 59% the rupture strain of CFRP) for the beams without anchors and from 9.5‰ to 14.5‰ (from 45% to 69% the rupture strain of CFRP) for those with anchors;
5. The strain increase of the tendons has a strong correlation with factors reflecting the CFRP sheet ratio and their actual strain with correlation factor  $CORR \geq 0.88$ . Moreover, the use of CFRP sheets reduced the compressive strain of concrete (up to 46% and 31% for the beams without and with anchors, respectively) and this reduction was inversely proportional to the CFRP sheet ratio;
6. The proposed equations for calculation of tendon strain increase of UPC beams strengthened with CFRP sheets allow to predict the flexural capacity with high accuracy and low variation (Mean =0.94 and COV =0.08).

It is strongly recommended to carry out more studies to provide the comprehensive understanding of the flexural behavior of CFRP strengthened UPC beams, particularly strengthened beams with mechanical and spike anchors.

## ACKNOWLEDGMENTS

This research was funded by Vietnam Foundation for Science & Technology Development (NAFOSTED) under Grant No. 107.99-2015.30.

## REFERENCES

- [1] Bakis C, Bank LC, Brown V, Cosenza E, Davalos J, Lesko J, Machida A, Rizkalla S, and Triantafillou T. Fiber-reinforced polymer composites for construction-state-of-the-art review. *J Compos Constr.* 2002;6:73-87.
- [2] Saadatmanesh H, and Ehsani M. RC Beams Strengthened with GFRP Plates: Part I: Experimental Study. *J Struct Eng.* 1991;117:3417-33.
- [3] Triantafillou TC, and Plevris N. Strengthening of RC beams with epoxy-bonded fibre-composite materials. *Mater Struct.* 1992;25:201-11.
- [4] Nanni A. Concrete repair with externally bonded FRP reinforcement. *Concr Int.* 1995;17:22-6.

- [5] Rabinovitch O, and Frostig Y. Experiments and analytical comparison of RC beams strengthened with CFRP composites. *Composites Part B: Engineering*. 2003;34:663-77.
- [6] Kotynia R, Abdel Baky H, Neale KW, and Ebead UA. Flexural strengthening of RC beams with externally bonded CFRP systems: Test results and 3D nonlinear FE analysis. *J Compos Constr*. 2008;12:190-201.
- [7] Attari N, Amziane S, and Chemrouk M. Flexural strengthening of concrete beams using CFRP, GFRP and hybrid FRP sheets. *Constr Build Mater*. 2012;37:746-57.
- [8] Reed CE, and Peterman RJ. Evaluation of prestressed concrete girders strengthened with carbon fiber reinforced polymer sheets. *J Bridge Eng*. 2004;9:185-92.
- [9] Rosenboom O, Hassan TK, and Rizkalla S. Flexural behavior of aged prestressed concrete girders strengthened with various FRP systems. *Constr Build Mater*. 2007;21:764-76.
- [10] Rosenboom O, Walter C, and Rizkalla S. Strengthening of prestressed concrete girders with composites: Installation, design and inspection. *Constr Build Mater*. 2009;23:1495-507.
- [11] Kim YJ, Green MF, and Fallis GJ. Repair of bridge girder damaged by impact loads with prestressed CFRP sheets. *J Bridge Eng*. 2008;13:15-23.
- [12] Di Ludovico M, Prota A, Manfredi G, and Cosenza E. FRP strengthening of full-scale PC girders. *J Compos Constr*. 2010;14:510-20.
- [13] Nguyen TTD, Matsumoto K, Sato Y, Iwasaki A, Tsutsumi T, and Niwa J. Effects of Externally Bonded CFRP Sheets on Flexural Strengthening of Pretensioned Prestressed Concrete Beams Having Ruptured Strands. *Journal of JSCE*. 2014;2:25-38.
- [14] Afefy HM, Sennah K, and Cofini A. Retrofitting Actual-Size Precracked Precast Prestressed Concrete Double-Tee Girders Using Externally Bonded CFRP Sheets. *J Perform Constr Facil*. 2016;30:04015020.
- [15] Kasan JL, Harries KA, Miller R, and Brinkman RJ. Limits of application of externally bonded CFRP repairs for impact-damaged prestressed concrete girders. *J Compos Constr*. 2014;18:A4013013.
- [16] Pino V, Nanni A, Arboleda D, Roberts-Wollmann C, and Cousins T. Repair of Damaged Prestressed Concrete Girders with FRP and FRCM Composites. *J Compos Constr*. 2017;21:04016111.
- [17] Chakrabari P. Behavior of un-bonded post-tensioned beams repaired and retrofitted with composite materials. *Structures Congress 2005: Metropolis and Beyond 2005*. p. 1-11.
- [18] El Meski F, and Harajli M. Flexural Behavior of Unbonded Posttensioned Concrete Members Strengthened Using External FRP Composites. *J Compos Constr*. 2013;17:197-207.
- [19] El Meski F, and Harajli M. Evaluation of the flexural response of CFRP-strengthened unbonded posttensioned members. *J Compos Constr*. 2015;19:04014052.
- [20] Ghasemi S, Akbar Maghsoudi A, Akbarzadeh Bengar H, and Reza Ronagh H. Sagging and hogging strengthening of continuous unbonded posttensioned HSC beams by NSM and EBR. *J Compos Constr*. 2016;20:04015056.
- [21] ACI 440.2R-17. Guide for the Design and Construction of Externally Bonded FRP Systems for Strengthening Concrete Structures. 4402R-17. Farmington Hills, MI: American Concrete Institute; 2017.
- [22] CNR DT200R1. Guide for the design and construction of externally bonded FRP systems for strengthening existing structures. CNR-DT200 R1/20132013.
- [23] TR 55. Design guidance for strengthening concrete structures using fibre composite materials. Camberley: Concrete Society; 2012.
- [24] Arduini M, and Nanni A. Parametric study of beams with externally bonded FRP reinforcement. *ACI Struct J*. 1997;94:493-501.
- [25] Garden H, and Hollaway L. An experimental study of the influence of plate end anchorage of carbon fibre composite plates used to strengthen reinforced concrete beams. *Compos Struct*. 1998;42:175-88.

- [26] Spadea G, Bencardino F, and Swamy R. Structural behavior of composite RC beams with externally bonded CFRP. *J Compos Constr.* 1998;2:132-7.
- [27] Bahn BY, and Harichandran RS. Flexural behavior of reinforced concrete beams strengthened with CFRP sheets and epoxy mortar. *J Compos Constr.* 2008;12:387-95.
- [28] Sobuz HR, Ahmed E, Uddin MA, and Sadiqul NM. Structural strengthening of RC beams externally bonded with different CFRP laminates configurations. *Journal of Civil Engineering (IEB).* 2011;39:33-47.
- [29] Ali A, Abdalla J, Hawileh R, and Galal K. CFRP mechanical anchorage for externally strengthened RC beams under flexure. *Physics Procedia.* 2014;55:10-6.
- [30] ACI 318-14. Building Code Requirements for Structural Concrete (ACI 318-14). Farmington Hills, Michigan, USA: American Concrete Institute (ACI); 2014.
- [31] Smith ST, and Teng JG. FRP-strengthened RC beams. I: review of debonding strength models. *Eng Struct.* 2002;24:385-95.
- [32] Teng JG, Chen JF, Smith ST, and Lam L. FRP-strengthened RC structures. Chichester, West Susses, UK: John Wiley and Sons; 2002.
- [33] Teng J, Smith ST, Yao J, and Chen J. Intermediate crack-induced debonding in RC beams and slabs. *Constr Build Mater.* 2003;17:447-62.
- [34] Maguire M, Chang M, Collins WN, and Sun Y. Stress Increase of Unbonded Tendons in Continuous Posttensioned Members. *J Bridge Eng.* 2017;22:04016115.
- [35] Tam A, and Pannell F. The ultimate moment of resistance of unbonded partially prestressed reinforced concrete beams. *Mag Concr Res.* 1976;28:203-8.
- [36] Au F, and Du J. Prediction of ultimate stress in unbonded prestressed tendons. *Mag Concr Res.* 2004.

## LIST OF FIGURES

- Fig. 1:** Unidirectional fabrics with carbon fibers
- Fig. 2:** Details of the tested beams
- Fig. 3:** Test setup
- Fig. 4:** Failure pattern of the tested beams
- Fig. 5:** Debonding and delamination of CFRP sheets
- Fig. 6:** Relative load –deflection relationships at mid-span of the tested beams
- Fig. 7:** Ratios of flexural capacities and ratios of mid-span deflections at failure of the strengthened beams to that of the reference beam
- Fig. 8:** Description of the calculation of the energy absorption capacity ( $E_b$ ) of the tested beams
- Fig. 9:** Relative load-crack width diagrams of tested beams
- Fig. 10:** Comparison of crack width of strengthened beams with that of the reference beam
- Fig. 11:** Relative load-strain diagrams of CFRP sheets and tendons
- Fig. 12:** Maximum strain increase of tendons in strengthened beams versus that in the reference beam
- Fig. 13:** Relation between ratio ( $\Delta\epsilon_{pu}/\epsilon_{fu}$ ) vs number of CFRP sheets
- Fig. 14:** Ratio of tendon yield force of the strengthened beams to that of the reference beam vs the number of CFRP layers
- Fig. 15:** Correlation between maximum strain increase of tendons and parameters of CFRP sheets
- Fig. 16:** Comparison of predicted and experimental flexural capacities

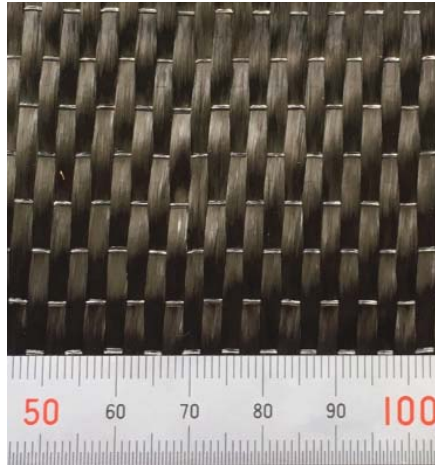
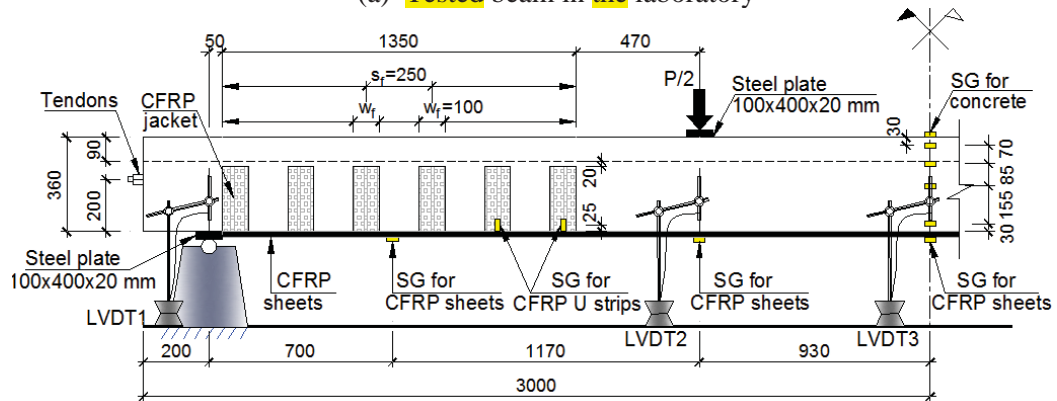


**Fig. 1:** Unidirectional fabrics with carbon fibers

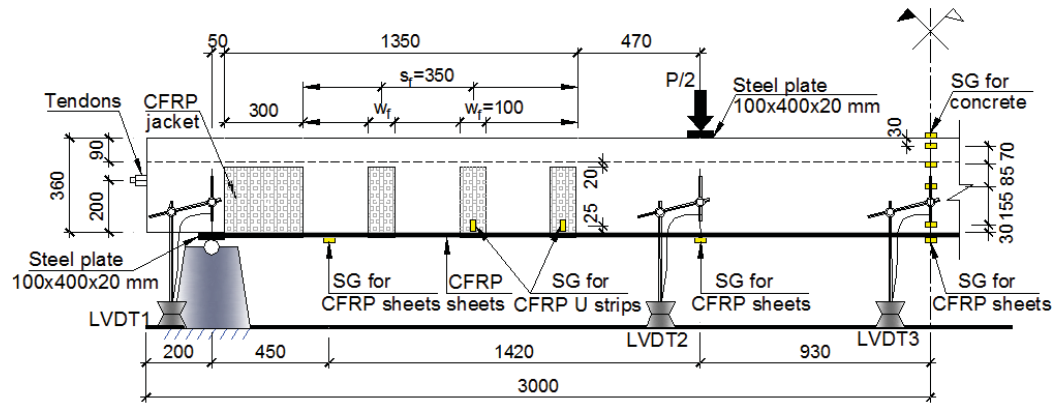
**Fig. 2:** Details of the tested beams



(a) Tested beam in the laboratory



(b) CFRP strengthening configuration and arrangement of strain gauges (SG) with type of CFRP U-wrapped anchorage AN1 system



(c) CFRP strengthening configuration and arrangement of strain gauges (SG) with type of CFRP U-wrapped anchorage AN2 system

**Fig. 3:** Test setup



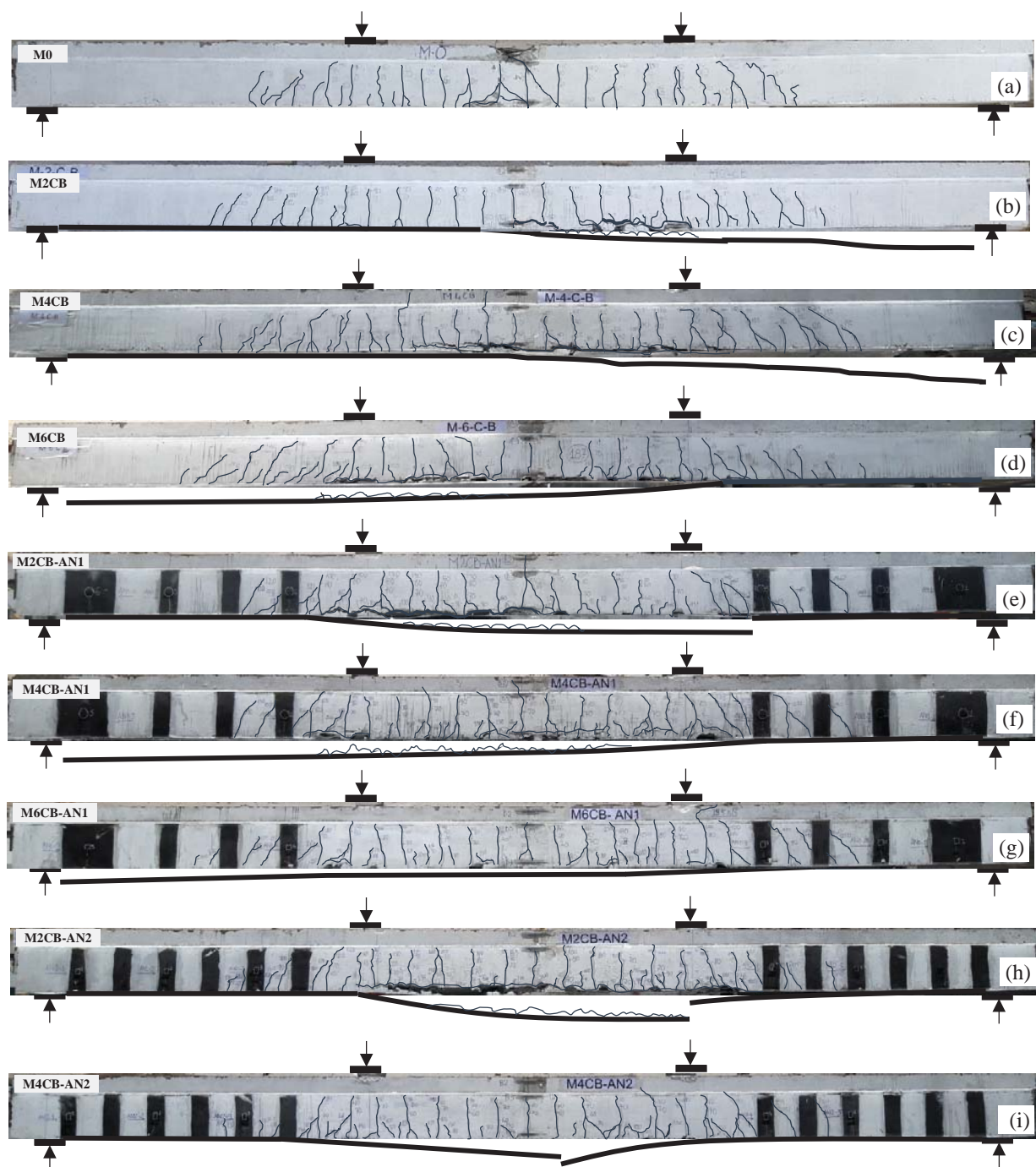
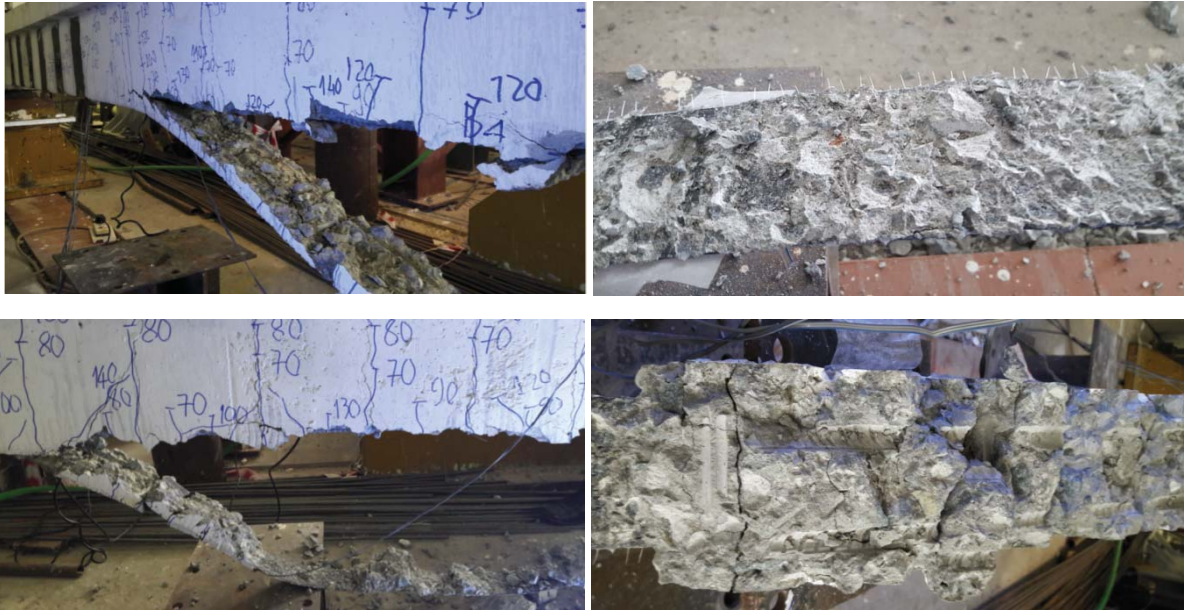


**Fig. 4:** Failure pattern of the tested beams





(a) Cover separation in the flexural span



(b) Interfacial debonding in the shear span

**Fig. 5:** Debonding and delamination of CFRP sheets

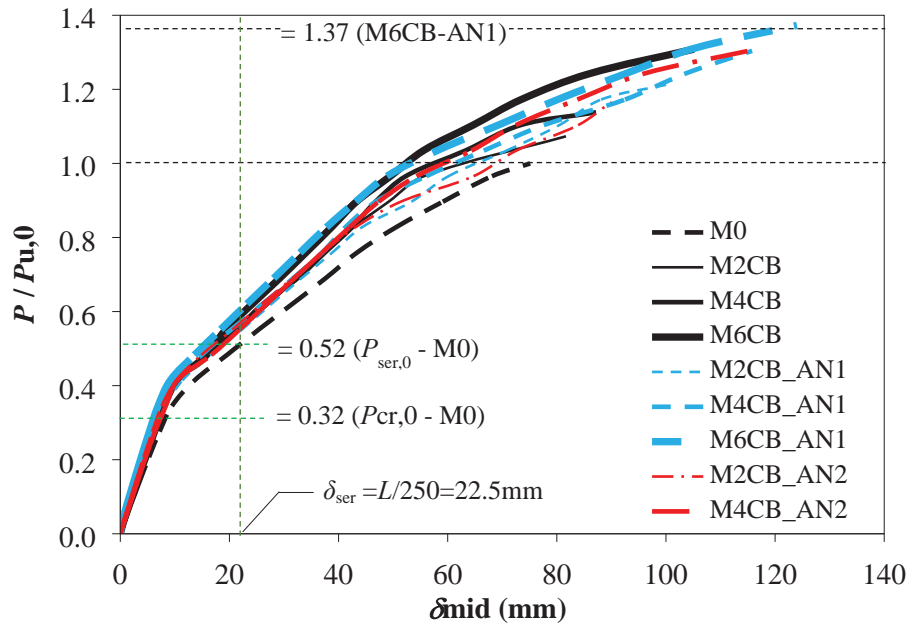
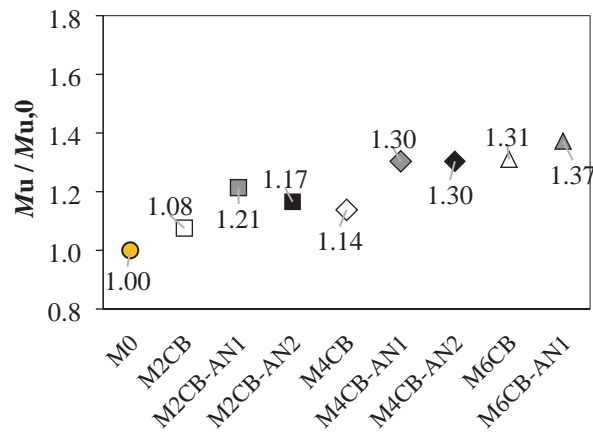
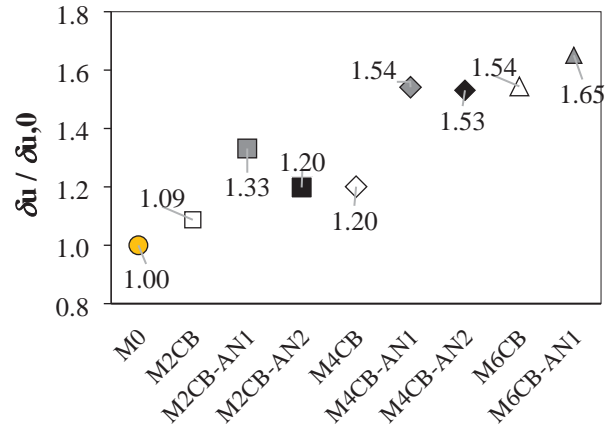


**Fig. 6:** Relative load-deflection relationships at mid-span of the tested beams



(a) Flexural capacity



(b) Mid-span deflection at the beam failure

Note: first character – monotonic loading (M); second character – number of CFRP layers (0, 2, 4, and 6); third character – FRP type (CFRP – C); fourth character – strengthening scheme (bending – B); AN1 or AN2 – type of CFRP anchorage U-wraps.

**Fig. 7:** Ratios of flexural capacities and ratios of mid-span deflections at failure of the strengthened beams to that of the reference beam

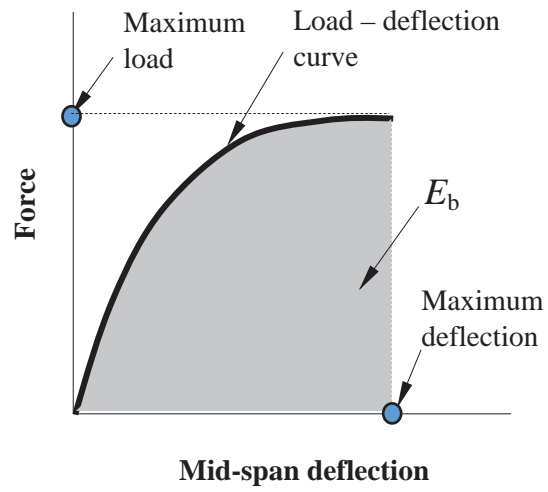


**Fig. 8:** Description of the calculation of the energy absorption capacity ( $E_b$ ) of the tested beams

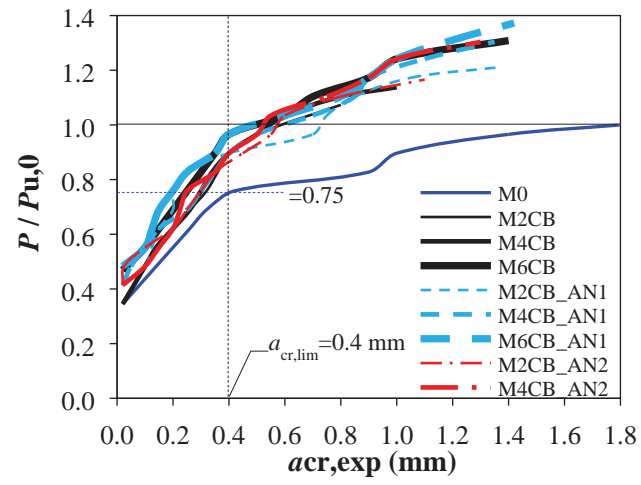
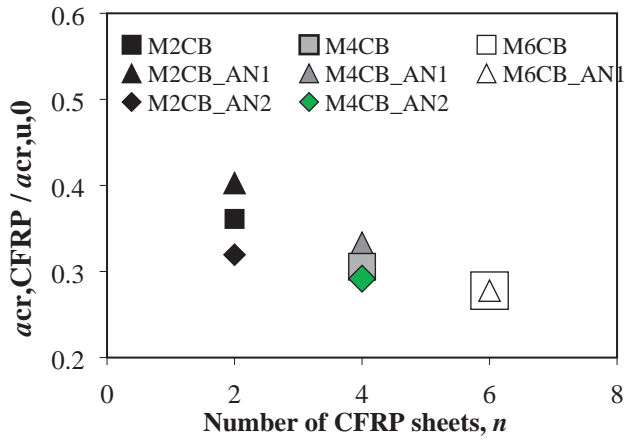
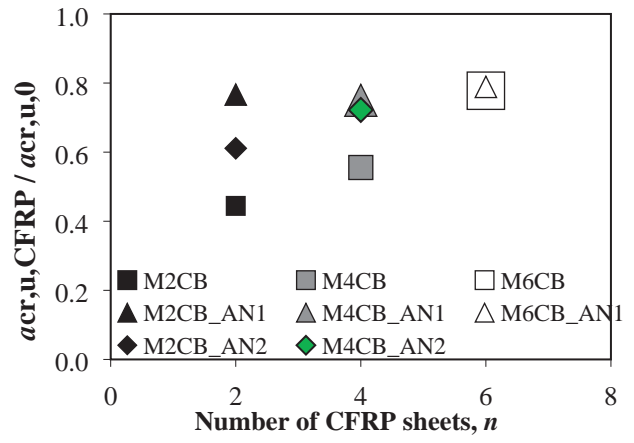


**Fig. 9:** Relative load-crack width diagrams of the tested beams

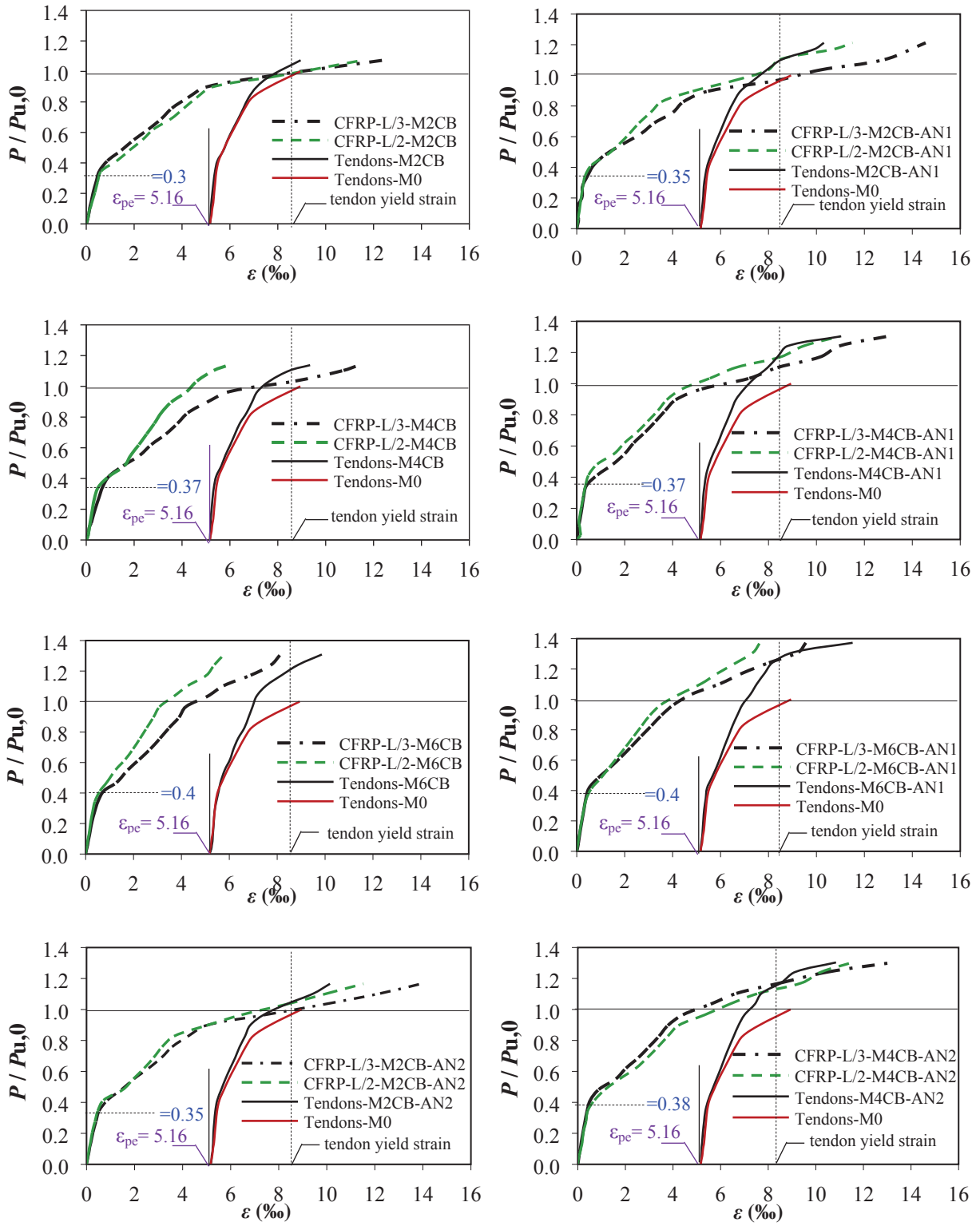


(a) at failure load of the reference beam –  $P_{u,0}$



(b) at failure load of the strengthened beams –  $P_{u,CFRP}$

**Fig. 10:** Comparison of crack width of the strengthened beams with that of the reference beam



Note: Symbols L/3 and L/2 show the locations of SGs on CFRP sheets, in which L is the effective span.

**Fig. 11:** Relative load-strain diagrams of CFRP sheets and tendons

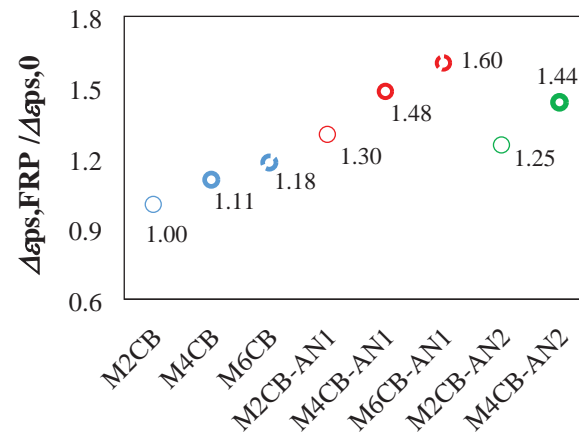


**Fig. 12:** Maximum strain increase of tendons in strengthened beams versus that **in the reference** beam



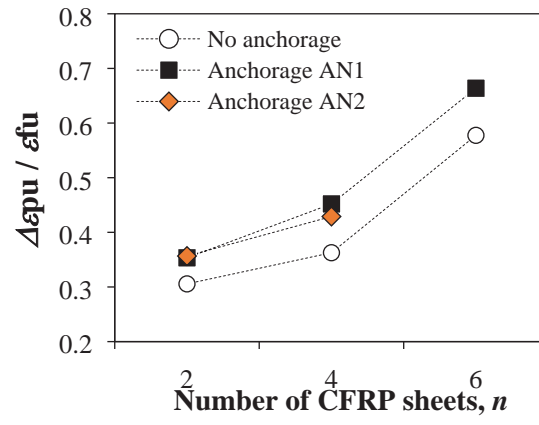


**Fig. 13:** Relation between ratio ( $\Delta\epsilon_{pu} / \epsilon_{fu}$ ) vs number of CFRP sheets

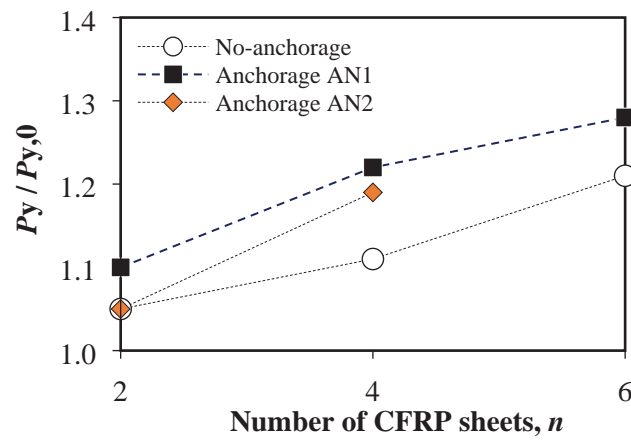


**Fig. 14:** Ratio of tendon yield force of the strengthened beams to that of the reference beam vs the number of CFRP layers

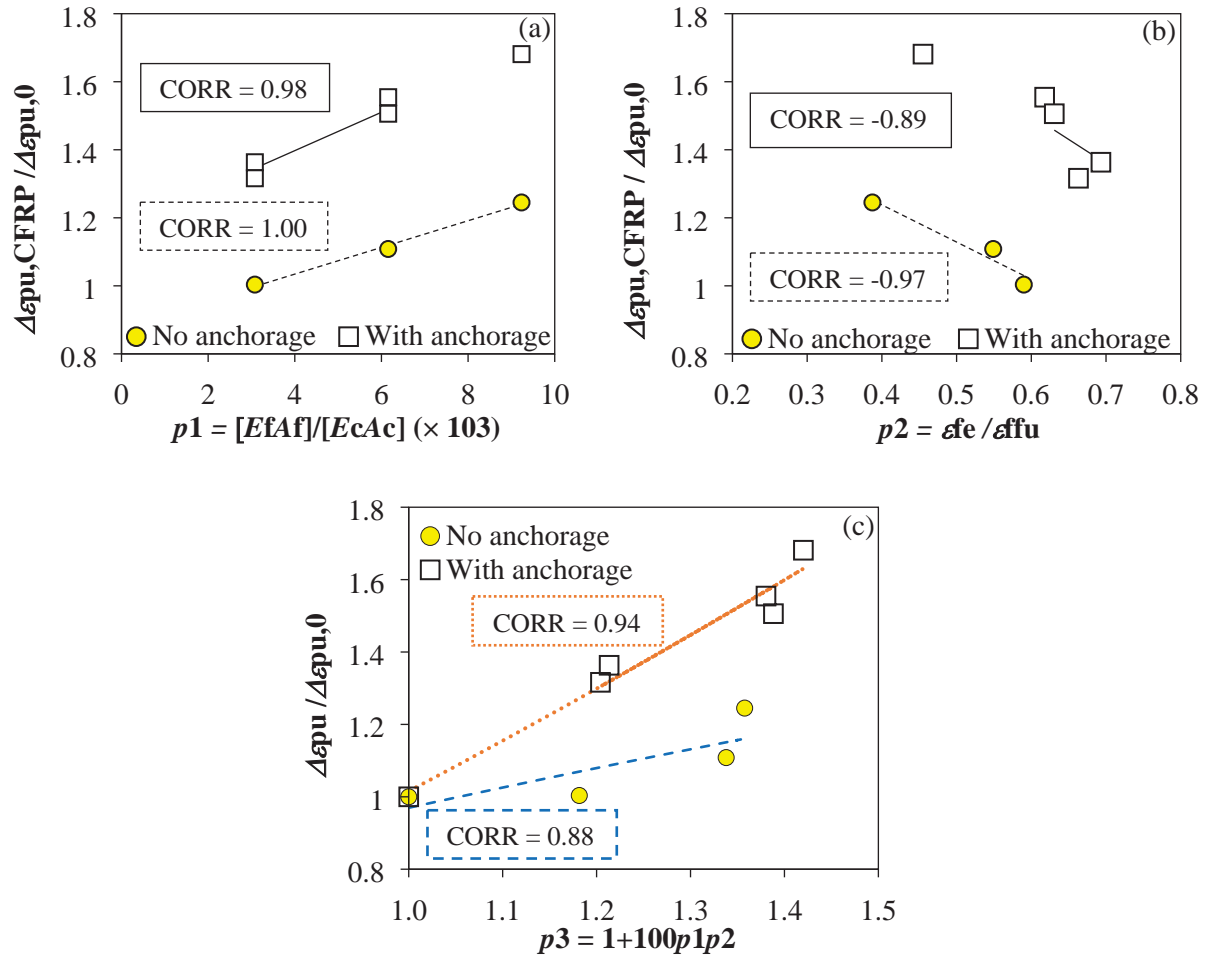
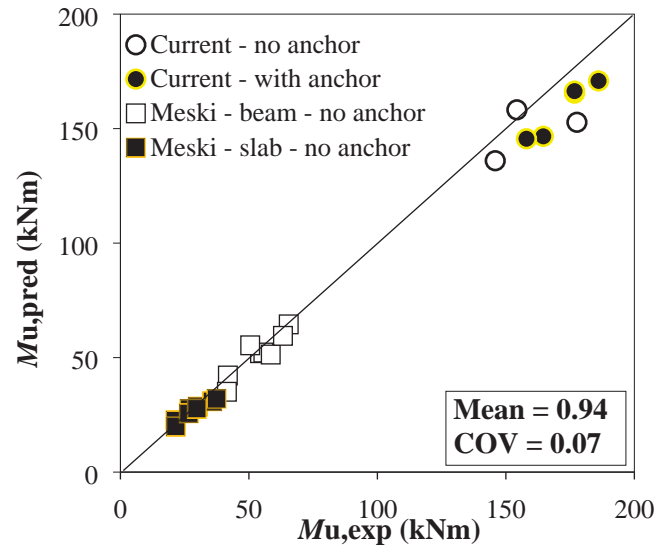


**Fig. 15:** Correlation between maximum strain increase of tendons and parameters of CFRP sheets



Note: Meski = El Meski and Harajli, 2013

**Fig. 16:** Comparison of predicted and experimental flexural capacities

## LIST OF SYMBOLS

$a_{cr,CFRP}$	: crack width of the strengthened beams at the failure load of the control beam, mm;
$a_{cr,exp}$	: crack width of the tested beams, mm;
$a_{cr,lim}$	: limit crack width, = 0.4 mm;
$a_{cr,u,0}$	: maximum crack width of the control beam, mm;
$a_{cr,u,CFRP}$	: maximum crack width of the strengthened beams, mm;
$a_f$	: width of flexural-strengthening CFRP sheets, mm;
$b$	: web width of beam, mm;
$b_f$	: flange width of beam, mm;
$b_w$	: web width of beam, mm;
$c$	: depth of concrete compressive zone, mm;
$d'$	: effective depth to compressive rebars, mm;
$d_f$	: effective depth of CFRP sheets, mm;
$d_p$	: effective depth to prestressing tendons, mm;
$d_s$	: effective depth to tensile rebars, mm;
$e$	: eccentricity of the prestressing force with respect to the centroid of the concrete section, mm;
$f_{c,cube}, f_{sp,cube}$	: mean compressive and splitting tensile strength of concrete cubes, respectively, N/mm <sup>2</sup> ;
$f_c'$	: nominal compressive strength of concrete cylinders, N/mm <sup>2</sup> ;
$f_{epoxy,u}$	: ultimate tensile strength of epoxy resin, N/mm <sup>2</sup> ;
$f_{fe}$	: stress in CFRP sheet, N/mm <sup>2</sup> ;
$f_{ffu}$	: ultimate tensile strength of carbon fiber fabric, N/mm <sup>2</sup> ;
$f_{pe}$	: effective prestressing stress in tendons, N/mm <sup>2</sup> ;
$f_{ps}$	: stress in tendon, N/mm <sup>2</sup> ;
$f_{py}, f_{pu}$	: yield and ultimate strength of tendons, respectively, N/mm <sup>2</sup> ;
$f_s, f_s'$	: stress in tensile and compressive rebar, N/mm <sup>2</sup> ;

$f_t$	: maximum concrete's tensile stress due to jacking force at prestress transfer stage determined according to <a href="#">ACI 318 (2014)</a> , N/mm <sup>2</sup> ;
$f_y, f_u$	: yield and ultimate strength of tensile rebars, respectively, N/mm <sup>2</sup> ;
$f_{yw}, f_{uw}$	: yield and ultimate strength of stirrups, respectively, N/mm <sup>2</sup> ;
$h$	: overall depth of beam, mm;
$h_f$	: thickness of beam flange, mm;
$n$	: number of CFRP <a href="#">sheet</a> layers;
$p_1$	: parameter reflecting effect of mechanical ratio of CFRP sheets, $= E_f A_f / (E_c A_c)$ ;
$p_2$	: parameter reflecting effect of working effectiveness of CFRP sheets, $= \varepsilon_{fu} / \varepsilon_{ffu}$ ;
$p_3$	: parameter reflecting effect of mechanical ratio and effect of working effectiveness of CFRP sheets, $= 1 + 100p_1p_2$ ;
$r$	: radius of gyration of the section, mm;
$r_{xy}$	: the sample Pearson correlation coefficient of two variable $x$ and $y$ ;
$s_f$	: spacing of CFRP U-wraps anchorage, mm;
$t_f$	: thickness of one ply of the CFRP sheet, mm;
$w_f$	: width of the CFRP U-wraps anchorage, mm;
$w_u$	: maximum crack width at beam failure, mm;
$y_b$	: distance from the centroid of the concrete section to the farthest bottom fiber, mm;
$A_c, A_f$	: cross-sectional <a href="#">al</a> area of concrete beam and CFRP sheets, respectively, mm <sup>2</sup> ;
$A_s, A'_s$	: cross-sectional <a href="#">al</a> area of tensile and compressive rebar, mm <sup>2</sup> ;
$A_p$	: cross-sectional <a href="#">al</a> area of tendons, mm <sup>2</sup> ;
$CORR$	: correlation coefficient;
$E_b$	: energy absorption capacity, Nmm;
$E_c, E_{epoxy}$	: modulus of elasticity of concrete and epoxy resin, respectively, N/mm <sup>2</sup> ;
$E_f, E_p, E_s$	: modulus of elasticity of carbon fiber fabric, tendons, and rebars, respectively, N/mm <sup>2</sup> ;
$I_c$	: <a href="#">second</a> moment of <a href="#">cross-sectional area</a> with respect to an axis passing its centroid, mm <sup>4</sup> ;

$F_p, F_{pi}$	: effective and initial prestressing force in tendons, respectively, kN;
$L_0, L$	: length and span of beam, respectively, mm;
$M_{DL}$	: moment due to dead load of beam, Nmm;
$M_u$	: flexural resistance of test beam, kNm;
$M_{u,0}$	: flexural resistance of <b>the reference</b> beam, kNm;
$M_{u,pred}$	: theoretical flexural resistance of test beam calculated according to <a href="#">ACI 440.2R (2017)</a> , kNm;
$M_{u,exp}$	: experimental flexural capacity of the beams, kNm;
$P$	: applied force, kN;
$P_{cr}$	: cracking force, kN;
$P_{cr,0}, P_{cr,CFRP}$	: flexural cracking force of control and CFRP strengthened beam, respectively, kN;
$P_{ser,0}$	: force of control beam at loading level corresponding to crack width, $a_{cr,lim}=0.4\text{mm}$ , kN;
$P_{ser}$	: <b>allowable load at the service state</b> , kN;
$P_u$	: maximum force, kN;
$P_{u,0}$	: maximum force of control beam, kN;
$P_{u,CFRP}$	: failure load of the strengthened beams, kN;
$P_y$	: yield force of tendons of CFRP strengthened beam, kN;
$P_{y,0}$	: yield force of tendons of control beam, kN;
$\alpha_1$	: multiplier on $f'_c$ to determine intensity of an equivalent rectangular stress distribution for concrete according to <a href="#">ACI 440.2R (2017)</a> ;
$\beta_1$	: ratio of depth of equivalent rectangular stress block to depth of the neutral axis according to <a href="#">ACI 440.2R (2017)</a> ;
$\delta_{mid}$	: midspan deflection of tested beams, mm;
$\delta_{ser}$	: <b>limit</b> deflection, $=L_0/250=22.5$ , mm;
$\delta_u, \delta_{u,0}$	: deflection of tested beams and control beam <b>at beam failure</b> , respectively, mm;

$\delta_{u,mid}$	: beam deflection at mid span at failure, mm;
$\Delta\epsilon_{ps,0}$	: strain increase of the tendons of the control beam, ‰;
$\Delta\epsilon_{ps,CFRP}$	: strain increase of the tendons of the strengthened beams, ‰;
$\Delta\epsilon_{pu}$	: maximum increase in strain of tendons of test beam, ‰;
$\Delta\epsilon_{pu,0}$	: maximum increase in strain of tendons of control beam, ‰;
$\Delta\epsilon_{pu,CFRP}$	: experimental maximum increase in strain of tendons of strengthened beam, ‰;
$\Delta\epsilon_{ps,CFRP}$	: strain increase in strain of unbonded tendons of CFRP-strengthened beam, ‰;
$\epsilon$	: strain, ‰;
$\epsilon_{bi}$	: initial substrate strain, ‰;
$\epsilon_c$	: compressive concrete strain determined according to ACI 440.2R (2017), ‰.
$\epsilon_{ccu}$	: maximum compressive concrete strain, ‰;
$\epsilon_{cu}$	: ultimate compressive concrete strain at failure, =3‰;
$\epsilon_{fd}$	: debonding strain, ‰;
$\epsilon_{fe}$	: effective strain of CFRP sheets, ‰;
$\epsilon_{ffu}$	: rupture strain of carbon fiber fabric, ‰;
$\epsilon_{fu}$	: maximum tensile strain of CFRP sheets at beam failure, ‰;
$\epsilon_{fu,an,aver}$	: average maximum tensile strain of CFRP U-strip anchorage at beam failure, ‰;
$\epsilon_{fu,L/3}, \epsilon_{fu,mid}$	: maximum tensile strain of CFRP sheets at loading point and midspan at beam failure, respectively, ‰;
$\epsilon_{p,u}$	: rupture strain of tendon (=0.035);
$\epsilon_{p,u,mid}, \epsilon_{p,u,end}$	: maximum tensile strain in tendons at the mid span and near the support at beam failure, respectively, ‰;
$\epsilon_{pe}$	: effective prestressing strain in tendons, = $F_p / (E_p A_p)$ , ‰;
$\epsilon_{pi}$	: initial strain in tendon, ‰;
$\epsilon_{ps,CFRP}$	: total strain in unbonded tendon of CFRP-strengthened beam, ‰;



- $\epsilon_{py}$  : specified yield strain in tendon,  $= f_{py} / E_p = 8.59\%$ ;
- $\epsilon_s, \epsilon'_s$  : strain for tensile and compressive rebar, %;
- $\epsilon_{su}$  : maximum tensile strain in rebars at beam failure, %;
- $\rho_f, \rho_p$  : reinforcement ratio of CFRP sheets and tendons, respectively, %;
- $\rho_s, \rho_{sw}$  : reinforcement ratio of tensile rebars and stirrups, respectively, %;
- $\psi$  : ratio of plastic concrete length to depth of concrete compressive zone.

## LIST OF TABLES

**Table 1:** Mechanical properties of the materials

**Table 2:** Summary of test parameters

**Table 3:** Test results

**Table 4:** The predicted and experimental flexural capacities

**Table 1:** Mechanical properties of the materials

Concrete		Tendons <sup>a</sup>			CFRP <sup>a</sup>			Longitudinal steel rebars			Steel stirrups	
$f_{c,cube}$ MPa	$f_{sp,cube}$ MPa	$f_{pu}$ MPa	$f_{py}$ GPa	$E_p$ %	$f_{ffu}$ MPa	$E_f$ GPa	$\varepsilon_{ffu}$ %	$f_u$ MPa	$f_y$ MPa	$E_s$ GPa	$f_{uw}$ MPa	$f_{yw}$ MPa
47.2	5.8	1860	1675	195	4900	240	2.1	600	430	200	463	342

Note: <sup>a</sup> Values provided by manufacturers.

**Table 2:** Summary of test parameters

Specimen	$b \times h \times b_f \times h_f \times L_0$ mm	$d_p$ mm	$\rho_s$ %	$\rho_{sw}$ %	$\rho_p$ %	$n$	$w_f$ mm	$s_f$ mm	$t_f$ mm	$a_f$ mm
M0	110×360×200×90×6000	305	0.47	0.29	0.41	0	-	-	-	-
M2CB						2	-	-	0.166	70
M4CB						4	-	-	0.166	70
M6CB						6	-	-	0.166	70
M2CB-AN1						2	300/100	250	0.166	70
M4CB-AN1						4	300/100	250	0.166	70
M6CB-AN1						6	300/100	250	0.166	70
M2CB-AN2						2	100	150	0.166	70
M4CB-AN2						4	100	150	0.166	70

**Table 3:** Test results

Beam	$P_{cr}$	$P_u$	$\delta_{u,mid}$	$\epsilon_{ccu}$	$\epsilon'_{fu,an,aver}$	$\epsilon'_{fu,L/3}$	$\epsilon'_{fu,mid}$	$\epsilon_{p,u,mid}$	$\epsilon_{p,u,end}$	$\epsilon_{su}$	$w_u$	$E_b$	Failure mode
	kN	kN	mm	%	%	%	%	%	%	%	mm	Nmm ( $\times 10^3$ )	
M0	46	145	75.1	3.5	-	-	-	8.9	-	33.5	1.8	7152	TY-MC
M2CB	49	156	81.7	1.9	-	12.4	11.5	8.9	8.9	11.6	0.8	8827	TY-LC-DB
M4CB	53	165	87.2	2.2	-	11.4	5.9	9.3	-	29.1	1.0	10438	TY-LC-DB
M6CB	58	190	105.1	2.7	-	8.1	5.7	9.8	9.0	32.0	1.4	13873	TY-LC-DB
M2CB-AN1	51	176	100	2.6	3.9	14.5	11.5	14.7	14.5	27.4	1.4	11753	TY-LC-R
M4CB-AN1	55	189	115.8	2.8	6.8	12.9	10.9	11.0	-	20.8	1.3	14994	TY-LC-RAN-DB
M6CB-AN1	58	199	124	3.0	7.2	9.5	7.6	11.5	11.5	19.4	1.4	17452	TY-LC-RAN-DB
M2CB-AN2	51	169	90.0	2.4	1.2	13.9	13.2	10.1	-	27.6	1.1	10065	TY-LC-R
M4CB-AN2	55	189	115.0	2.5	4.7	11.5	11.5	10.8	10.8	-	1.3	15029	TY-LC-R

Note: TY - tendon yielding; MC – concrete crushing at midspan; LC – local crushing of concrete; R – rupture of CFRP sheets; RAN – rupture of CFRP U-strips anchorage system; DB – debonding of CFRP sheets.

**Table 4:** The predicted and experimental flexural capacities

Specimen	$f_c'$	$b_w$	$d_p$	$d_s$	$L_0$	$\psi$	$\varepsilon_{cu}$	$c$	$\varepsilon_{ps,CFRP}$	$\varepsilon_{fe}$	$M_{u,pred}$	$M_{u,exp}$	$M_{u,pred}/M_{u,exp}$
	MPa	mm	mm	mm	mm		‰	mm	‰	‰	kNm	kNm	
<i>FRP-strengthened UPC precracked beams (El Meski and Harajli, 2013)</i>													
UB1-H-F1	36	150	200	220	3250	9.8	2.2	53	6.2	8.4	42.2	41.8	1.01
UB1-H-F2	36	150	200	220	3250	9.8	2.1	66	6.2	6.0	51.9	54.3	0.96
UB1-P-F1	36	150	200	220	3250	9.8	2.2	53	6.3	8.4	35.1	41.4	0.85
UB1-P-F2	37	150	200	220	3250	9.8	2.0	64	5.2	6.0	52.2	55.6	0.94
UB2-H-F1	36	150	200	220	3250	9.8	3.0	67	6.3	8.4	55.4	50.5	1.10
UB2-H-F2	37	150	200	220	3250	9.8	2.6	78	6.0	6.0	64.5	65.5	0.99
UB2-P-F1	36	150	200	220	3250	9.8	3.0	67	6.4	8.4	51.3	58.5	0.88
UB2-P-F2	37	150	200	220	3250	9.8	2.6	78	6.1	6.0	59.5	63.3	0.94
US1-H-F1	36	360	85	92.5	3250	9.8	2.4	27.1	5.2	8.4	22.6	21.4	1.05
US1-H-F2	36	360	85	92.5	3250	9.8	2.2	33.4	5.4	6.0	27.6	26.9	1.03
US1-P-F1	36	360	85	98.5	3250	9.8	2.4	27.3	5.4	8.4	19.9	21.6	0.92
US1-P-F2	37	360	85	98.5	3250	9.8	2.2	33.0	5.5	6.0	28.6	30.1	0.95
US2-H-F1	36	360	85	92.5	3250	9.8	3.0	34.3	5.3	7.8	25.7	26.6	0.97
US2-H-F2	37	360	85	92.5	3250	9.8	2.7	38.7	4.9	6.0	31.0	35.8	0.87
US2-P-F1	36	360	85	98.5	3250	9.8	3.0	34.4	5.3	7.8	27.7	29.8	0.93
US2-P-F2	37	360	85	98.5	3250	9.8	2.8	39.4	5.2	6.0	32.0	37.4	0.85
Mean													<b>0.95</b>
Coefficient of Variation (COV)													<b>0.08</b>
<i>FRP-strengthened UPC non-cracked beams (Current study)</i>													
M2CB	38	110	304	329	6000	21.4	2.7	66	7.8	12.4	136.0	145.9	0.93
M4CB	38	110	304	329	6000	21.4	2.9	75	8.2	11.5	158.2	154.3	1.03
M6CB	38	110	304	329	6000	21.4	2.3	82	7.5	8.1	152.8	177.7	0.86
M2CB-AN1	38	110	304	329	6000	21.4	3.0	75	8.6	14.6	146.6	164.6	0.89
M4CB-AN1	38	110	304	329	6000	21.4	3.0	87	8.6	13.0	165.5	176.7	0.94
M6CB-AN1	38	110	304	329	6000	21.4	2.8	84	8.6	9.6	170.8	186.1	0.92
M2CB-AN2	38	110	304	329	6000	21.4	3.0	74	8.6	13.9	145.6	158.0	0.92
M4CB-AN2	38	110	304	329	6000	21.4	3.0	88	8.6	13.2	166.4	176.7	0.94
Mean													<b>0.93</b>
Coefficient of Variation (COV)													<b>0.05</b>
<b>Mean (all beams)</b>													<b>0.94</b>
<b>Coefficient of Variation (COV) (all beams)</b>													<b>0.07</b>

Note:  $\varepsilon_{fe}$  is the actual strain of CFRP sheets at the maximum load, which was adopted directly from the tests results.